Design and characterization of a linear position transducer based on Giant Magneto Resistance (GMR) effect.

Igor Tchertkov[♣], Duane Christy[♥] and Fred Parsons[♥]

[♥]Federal Products Co., 1144 Eddy St., Providence, RI 02905

[♣]Microcosm Technologies, Inc. 215 First St., Cambridge, MA 02142

In this report we describe a new linear position transducer based on the giant magneto resistance (GMR) effect. The GMR effect is a phenomenon observed in multilayer structures consisting of ferromagnetic, antiferromagnetic and paramagnetic metal films. The transducer consists of four GMR elements configured in a Wheatstone bridge with 380 Ohms nominal resistance of each leg. GMR elements were subjected to a high-gradient magnetic field created by specially designed Ne-Fe-B permanent magnets. A movable magnetic assembly was attached to a probe, the linear position of which was varied. This design represents an absolute, analog, linear position sensor.

The dimensions of each sensitive element were 35 x 3 x 2 mm and the whole transducer was packaged in a 12 x 2 x 2 cm housing. The sensitivity of the sensor was approximately 1 Ohm/mm. The best achieved deviation from linearity over a range of 23 mm was $\pm$ 10 μm (0.05% of full scale), with hysteresis of 5 μm. Noise density of the transducer was 60 $nV_{rms}/\sqrt{Hz}$, which allows 0.2 μm resolution with a 4 Hz update rate. The transducer possesses some temperature dependence. Each element of the bridge has temperature dependence around 2200 ppm/^oC which scales to 34 μm/^oC at the ends of the range of the full bridge.

Non-uniformity of the thickness of layers in the GMR structures, defects and inhomogeneity in metal films are discussed as possible causes of non-linearity, hysteresis, relaxation and noise observed in some samples.

Keywords: transducer, sensor, GMR, metrology, thin film

Introduction

The dimensional measurement community is always looking for new transducer technologies that would allow construction of new linear position sensors with better metrological characteristics for less cost than existing sensors.

Portable dial electronic indicators find applications in many sectors of industry. As of today, general-purpose indicators usually provide 1 μm resolution with ranges between 0.1 cm and 3 cm. They usually cost around 200-300 dollars and run on batteries for about a year. There are more accurate, higher resolution, longer range instruments which, of course, much more expensive and consume more power. All indicators in this group are scales based. Usually more accurate, higher resolution instruments utilize better and more expensive scales. They also tend to use more intensive signal processing which brings up both cost and power consumption.

In this paper we describe an attempt to design an inexpensive analog transducer with accuracy on the level of 1 μm, resolution about 0.1 μm, and range 25 mm. We choose very promising giant magneto resistive (GMR) effect as a transduction method.

The GMR is a relatively newly discovered phenomenon[1] observed in structures consisting of several magnetic and non-magnetic layers. Many systems were investigated during last decade with reported ΔR/R ratio up to 65% at room temperatures[2,3]. High GMR ratio in those systems was achieved on the expense of high values of magnetic field required for their operation. Dieny et. al.[4] reported in 1991 about very high GMR effect observed in more complex structures dubbed as "spin valve", consisting of uncoupled ferromagnetic and antiferromagnetic layers separated by non-magnetic metallic layers. These spin valve structures exhibit large GMR ratio and require small (on the order of several Oersteds) magnetic field to operate. Overall GMR effect is roughly an order of magnitude stronger than anisotropic magneto resistance (AMR) effect which makes it very attractive for sensor designers[5, 6, 7, 8].

Design of a linear position transducer

GMR effect in the multilayer structures

GMR resistors used in our transducers were spin valve structures designed, manufactured and characterized by Nonvolatile Electronics Inc., Eden Prairie, MN. The principle of operation of these structures is depicted in the Figure 1.

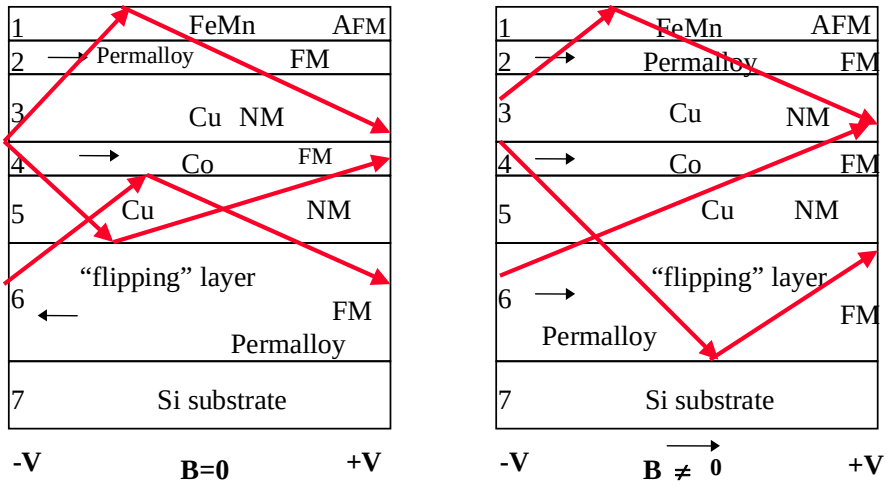

(a) High Resistance State (b) Low Resistance State

Figure 1. Spin valve GMR structure in the absence of external magnetic field (a) and in the presence of external field (b). Arrows drawn in layers 2, 4 and 6 represent the magnetization of a particular layer. Broken arrows represent the trajectories of electrons when dc voltage is applied along layers. Case (a) is a "low resistance state"; case (b) is a "high resistance state"

Occurrence of the GMR effect can be described as following[9, 10].

Soft magnetic layer 6, made, for example, from permalloy is a “flipping” layer, i.e., its magnetization is reversible under application of a proper external magnetic field. It is a relatively thick layer, about 70 Å. This layer is strongly anti-ferromagnetically coupled with hard magnetic layer 4 made, for example, from Co. This specific coupling is achieved by controlling the thickness of a “buffer” layer 5 made from Cu. This later has the thickness of the order of 15 Å. Layer 6 is also coupled, although somewhat weaker, with magnetic layer 2. This coupling is ferromagnetic. It is achieved again by controlling the thickness of another Cu buffer layer 3. Magnetically soft permalloy layer 2 is strongly coupled with anti-ferromagnetic layer 1 (which can be made from FeMn). In a sense anti-ferromagnetic materials are the hardest magnetic materials, because their net magnetization is zero and they are completely insensitive to external magnetic fields. Consequently, pinning in such a way the magnetization of the layer 2, permits operation under stronger external fields avoiding switching the pin layers.

In the absence of external magnetic field anti-ferromagnetic coupling between flipping layer 6 and pinning layer 4 prevails and magnetization of layer 6 is anti-parallel to the magnetization of layer 4, Figure 1 (a). Application of external field, Figure 1(b), flips the magnetization of the layer 6. The field needed for this permutation is determined by the difference in energy between mentioned above anti-ferromagnetic and ferromagnetic coupling. This difference can be made quite small, so that device will be sensitive to weak fields. This is in contrast to early GMR structures which required very strong magnetic fields.

Now consider electrical properties of such structures. To minimize energy, the majority of the electron spins in the ferromagnetic materials are oriented parallel to the magnetization vector ***M.*** When an electric field is applied, the spin-oriented conduction electrons accelerate until they encounter a scattering centers, which is, of course, the origin of the electrical resistivity. The average distance the conduction electrons accelerate through is called the coherence length. Consider the case in which the scattered electron travels the interlayer of a non-magnetic metal. Provided that thickness of this buffer layer is less than the coherence length, the conduction electron arrives at the interface of the adjacent ferromagnetic layer still carrying its original spin orientation. When this adjacent magnetic layer is magnetized in a parallel manner, the arriving electron has a high probability of entering the adjacent layer with negligible scattering, because it’s spin orientation matches that of that layer. On the other hand, when the adjacent layer is magnetized in an anti-parallel manner, the arriving electrons suffer strong scattering at the interface.

GMR ratio is defined as:

$$K_{GMR} = \frac{\Delta R_{GMR}}{R} = \frac{R_{\uparrow} - R_{\downarrow}}{(R_{\uparrow} + R_{\downarrow})/2}, \qquad (1)$$

where $R_{\uparrow}$ and $R_{\downarrow}$ are resistance of the GMR element, when the layer with reversible magnetization is completely magnetized in one direction, $R = (R_{\uparrow} + R_{\downarrow})/2$ is the nominal resistance of the whole device.

Principle of displacement sensing

Principle of displacement sensing is presented on the Fig. 2. It shows GMR stripe oriented along the axis of sensing. Movable magnet assembly is attached to the probe (not shown), displacement of which has to be measured. Permanent magnets (Nd-Fe-B) create magnetic field with high gradient region located along the centerline of magnets. Configuration of the magnetic field is such that, presumably, only one domain wall exists in the flipping layer of the GMR stripe. On the same time, magnetic field is not strong enough to cause re-magnetization of the pin layers. This magnetization was created during fabrication of the structure and

should remain intact for the life of the sensor. The domain wall separates two domains with anti-parallel magnetization. Left-hand domain has low resistance, because the magnetization in the flipping layer is parallel to the one in the pin layers. Right-hand domain has high resistance, because flipping layer and pin layers have anti-parallel magnetization. When magnet assembly has been displaced to the new position, length of left-hand and right-hand domains changes correspondingly, which causes the change in the total resistance of the element. When magnets are at the left-hand edge of the transducer, it has the highest resistance $R_{\uparrow}$, at the right-hand edge transducer has its lowest resistance $R_{\downarrow}$.

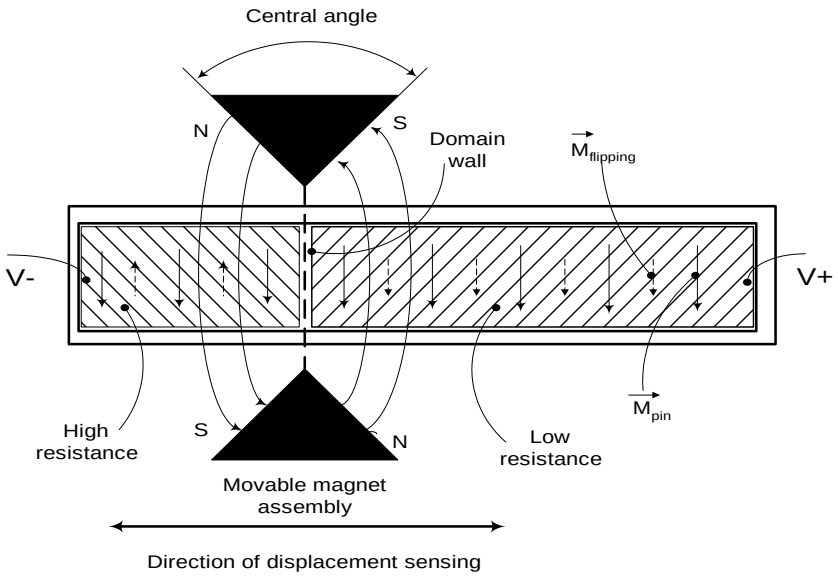

Figure 2. Schematic principle of operation of the GMR-based linear position transducer. Shadowed area is the GMR strip. Magnetization of pin layers and flipping layer is shown. Domain wall separates domains on the GMR stripe. If external voltage is applied, then left-hand domain has high resistance and right-hand domain has low resistance. Total resistance of the element is a linear function of magnet assembly position.

In order to increase signal-to-noise ratio and decrease susceptibility to temperature variations, four identical GMR resistors were configured into Wheatstone bridge. Wire bonding by standard IC technique was done at Honeywell's Technology Center. The cross-section of the transducer is shown in the Figure 3. The photograph of the working device is shown in Figure 4.

Model

Several physical effects determine the behavior of the transducer. Its transfer function can be written as

$$TF = \frac{X_{out}}{X_{in}} \qquad (2)$$

where ***TF*** is affected by temperature, direction of motion, speed of probe movement, etc. and also is a parametric function of many design variables, such as GMR and AMR coefficients, nominal resistance, geometrical dimensions, magnetic field characteristics and so on. A comprehensive model of the transducer

is hard to construct and it would be so difficult to use, that it is not worth it. We will present here a greatly simplified model which, however, describes the most important features of the transducer correctly.

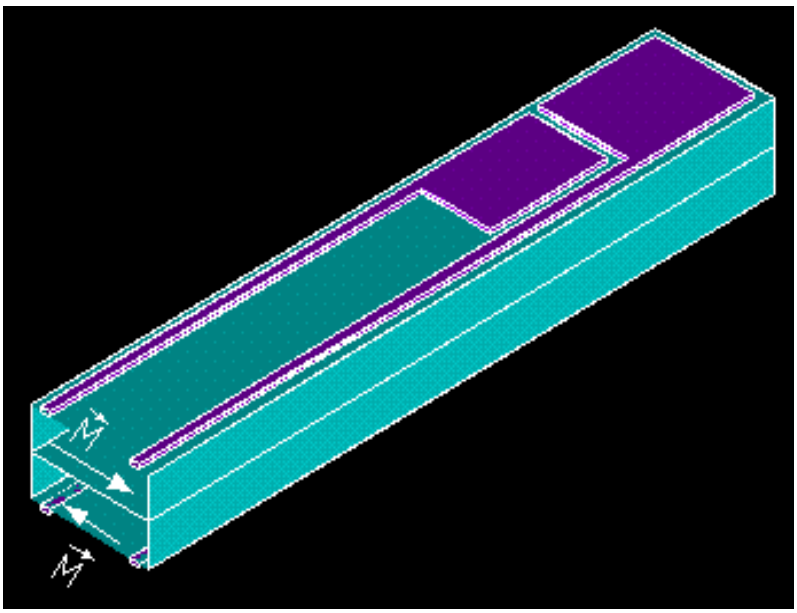

Figure 3. Cross-section of the GMR-based linear position transducer. It consists of four GMR resistors configured in Wheatstone bridge. Two elements were diced from 4" Si wafer and sandwiched botom-to-botom. Each dice has two GMR stripes. Magnetization of pin layers in each dice is shown. Dimensions of the sensor are (35 x 3 x 2) mm.

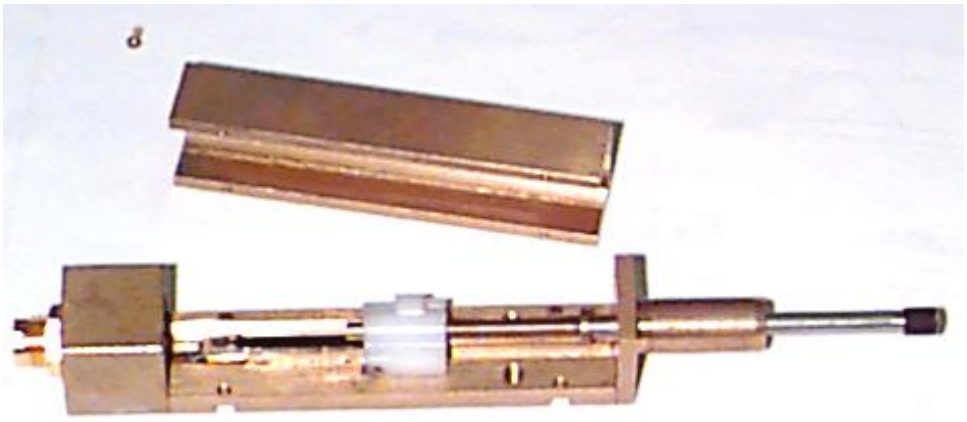

Figure 4. Photograph of the working prototype, manufactured by Federal Products Co.

It is assumed that in the flipping layer there are only two domains with antiparallel magnetization. These domains are separated by the domain wall, located along the line joining the centers of two magnets. Under normal operation conditions these two domains and a domain wall are always exist in GMR resistors.

Magnetic field configuration was modeled on finite element analysis system ANSYS™ Muliphysics 5.4. Figure 5(a) shows 2D magnetic field flux lines when the centerline of the magnet assembly was positioned at the edge of the range. Figure 5(b) and (c) show respectively the normal to the axis of the transducer component of the magnetic field $B_y(x)$ as a function of longitudinal coordinate x and a square of this component $B_y(x)^2$.

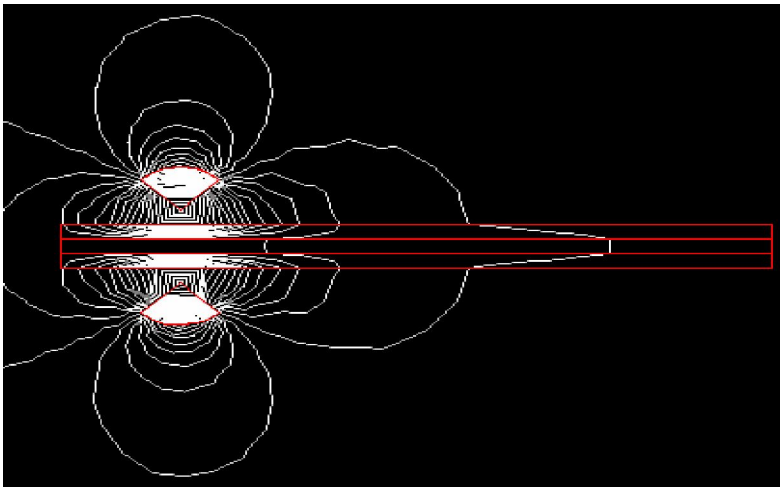

(a)

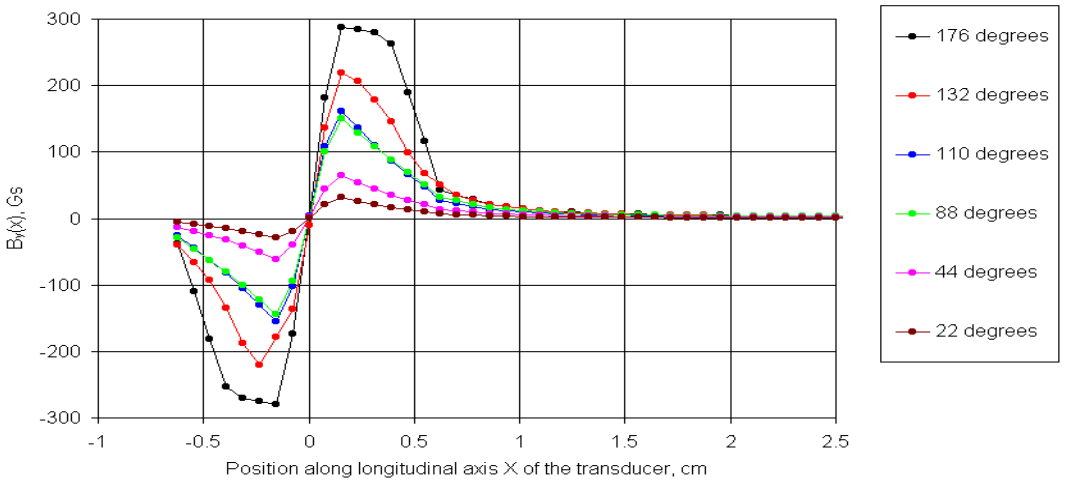

(b)

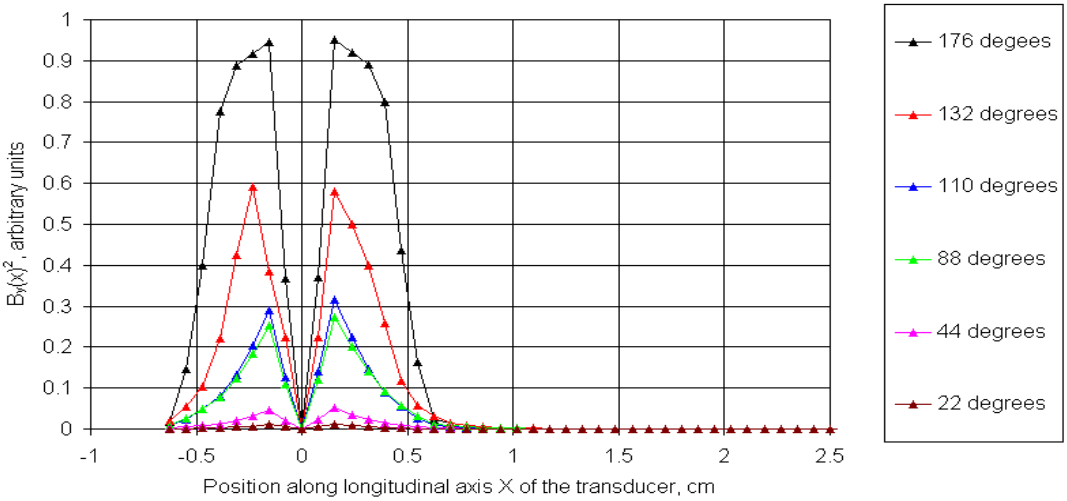

(c)

Figure 5. Results of the modeling on finite element analysis system ANSYS™ Multiphysics 5.4. (a) -- 2D magnetic field flux lines. Magnets with 88° central angle were positioned at the edge of the working range. A contour of a dice with two GMR stripes is shown. (b) -- $B_y(x)$ is a component of the magnetic field perpendicular to the axis of the sensor. Central angle is a parameter.(c) -- $B_y(x)^2$.

It can be shown that due solely to GMR effect the voltage measured across the bridge (V_{out}) is a linear function of displacement Δx measured from the center position (where bridge is balanced and V_{out} =0).

$$V_{out} = I_{in} \frac{R * K_{GMR}}{L} \Delta x \quad , \tag{3}$$

or

$$V_{out} = I_{in} R_{eff} (\Delta x) \tag{4}$$

where $\boldsymbol{I_{in}}$ is the constant current provided by power supply, $\boldsymbol{L}$ is the length of the sensor and $\boldsymbol{R_{eff}(\Delta x)}$ is the some effective resistance equal to $\frac{R * K_{GMR}}{L} \Delta x$

The situation is, however, more complicated because all conductors subjected to magnetic field, experience anisotropic magneto resistive (AMR) effect. Greatly simplified the AMR effect can be described as following. In contrast to the $\boldsymbol{B=0}$ case when trajectories of electrons between collisions are straight lines, application of the magnetic field bends trajectories causing increased number of collisions and increase of resistance. This effect of Lorentz force acting on carriers is compensated in long samples by the Hall voltage. Exact compensation happens only for electrons with some average velocity. However, the velocity of the ensemble of electrons is distributed around this average value. As a result, the trajectories of electrons are still somewhat disturbed, that gives rise to additional resistivity. The effect is maximum when $\boldsymbol{B}$ is perpendicular to current $\boldsymbol{J}$ and should decrease to zero when $\boldsymbol{B}$ is parallel to $\boldsymbol{I}$. Additional AMR contribution to resistance of the sample is proportional[11] to its resistance R:

$$\Delta R_{AMR} \propto R R_H{}^2 \left| I \times B \right|^2 \quad , \tag{5}$$

where R_H is the Hall constant.

When four nominally identical resistors forming a Wheatstone bridge subjected to the identical magnetic field, the net AMR contribution to the effective resistance should be equal to zero. In our situation it happens only when magnets are in the central position. At this position bridge is balanced and its effective resistance is zero. When magnets have been displaced from central position, R_{eff} in Eq. (4), is not zero any longer and V_{out} will contain some additional AMR contribution.

Our sensor has substantial length and all parts of the resistors "see" different magnetic field. In order to calculate total AMR contribution, the integral should be taken along the axis of the transducer. The following expression takes into account both GMR and AMR contributions to the sensor output:

$$V_{out} = I_{in} \frac{R * K_{GMR}}{L} \Delta x + (I_{in} \frac{R * K_{GMR}}{L} \Delta x) K_{AMR} \int_0^l B_y{}^2 (l, \Delta x) dl \quad , \tag{6}$$

where $K_{AMR} = \frac{\Delta R_{AMR}}{R}$ is usually on the order of 1-2%. Integral in this expression is a parametric function of Δx, which is a position of magnet assembly measured from the center of sensor. Figure 6 (a) shows AMR contribution as a function of magnet position with central angle of magnets as a parameter. It can be seen that while magnet assembly moves well inside the working range of transducer, the AMR contribution to the total resistance of the sensor is pretty much constant regardless of the shape of magnets. However, at the edges of the range some portions of resistors seized being subjected to magnetic field and AMR contribution to the total resistance decreases. It is clearly happens earlier for larger magnets. The more so, effect for larger magnets should be bigger. The modeled transducer output is shown in Figure 6 (b). In contrast to AMR contribution, the GMR portion is determined only by the position of the domain wall, thickness of which is a microscopic quantity, and therefore, GMR contribution to total resistance should vary linearly with displacement[12].

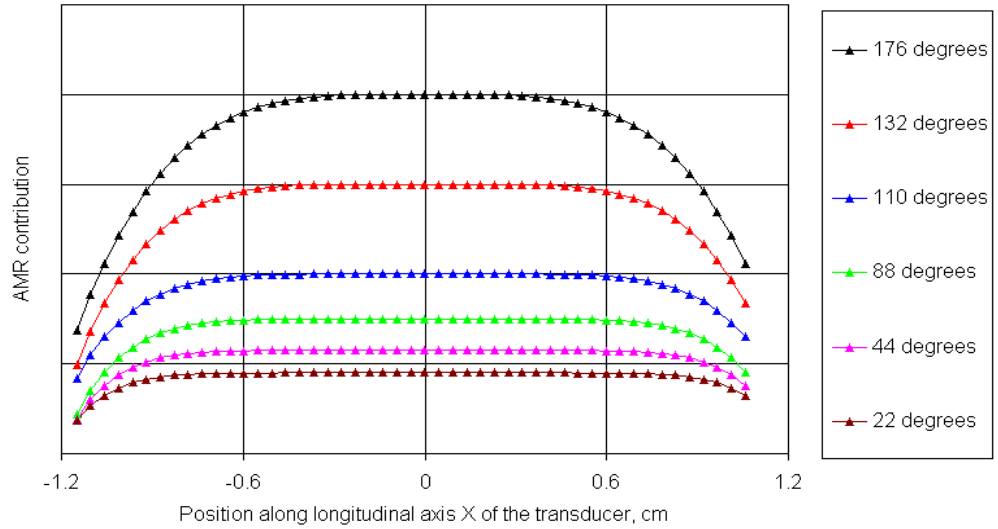

(a)

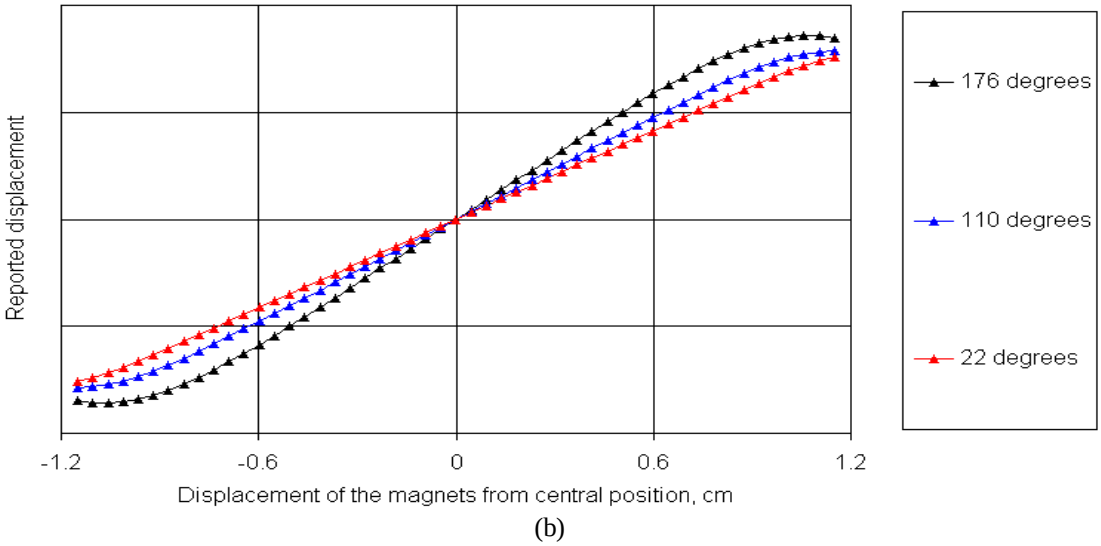

(b)

Figure 6. (a) Modeled AMR contribution to the total resistance of the transducer as a function of the magnets position. Zero position corresponds to the middle of the GMR stripe. (b) -- Modeled output of the GMR-based transducer. Both GMR and AMR effects are taken into account. Central angle is a parameter.

Hysteresis is hard to model quantitatively due to complex nature of the effect. Also, it requires more accurate knowledge of microstructure of GMR films. One estimate for the expected hysteresis can be obtain if we suppose that GMR films although being continuous are actually a conglomerate of micro grains which switch their magnetization independently. Now suppose that magnets just passed by one of those grains and switched its magnetization. Then if we stop and begin to move in opposite direction, this particle will not switch immediately -- it will "wait until it sees" magnetic field equaled to coercive force H_c and pointing in opposite direction. Knowing gradient of the magnetic field, Fig. 5 (b), in the central areas of magnet assembly and H_c for our GMR films (≈10 Oe) we can estimate expected hysteresis. The higher the gradient the smaller is the expected hysteresis. For 176^o, 132^o, 110^o, 88^o, 44^o and 22^o magnets we obtain hysteresis values 9, 12, 15, 16, 37 and 78 μm, respectively. Magnets with larger central angle produce the field with higher gradient and, therefore, hysteresis in such devices should be smaller.

In the truly continuos GMR films grains are strongly coupled and do not switch independently. Therefore, coercivities are low and hysteresis will be much smaller. In this case there is always a single, well-defined domain wall in the film. Magnetic field required to move this domain wall is much smaller than magnetic field required to create many walls in many grains or to switch the magnetization in the grains independently.

AMR effect also can contribute to the hysteresis in the following way. Hysteresis due to GMR effect means that there is a small difference in the resistance of the device depending upon the direction of movement. This small difference in the resistance factor (R) in the second (AMR) term in Eq. (6) gives rise to additional hysteresis due to AMR effect. As we discussed earlier hysteresis is smaller for magnets with larger central angle. This term, however, is proportional to magnetic field which is stronger for magnets with larger angle. Thus, varying central angle of the magnets one can hope to find a values for this parameter such that total hysteresis will be at minimum.

Temperature dependence of the transducer response can be derived from Eq. (6) and (4) and described by $\boldsymbol{R_{eff} = R_{eff}(T)}$ equation. Ignoring second order terms we get:

$$V_{out}(T) = I_{in}\frac{R(T) * K_{GMR}(T)}{L}\Delta x, \tag{7}$$

where

$$R(T) = R_0[1 + \alpha_R(T - T_0)], \tag{8}$$

is a familiar temperature dependence for metals with thermal coefficient of resistivity $\boldsymbol{\alpha_R}$. It is shown[3] that GMR ratio decreases quasi-linearly with increase of the temperature:

$$K_{GMR}(T) = K_{GMR0}[1 - a_{GMR}(T - T_0)] \tag{9}$$

with $\alpha_{GMR} \approx 0.0017$ 1/C.

Using Eq. (7), (8) and (9), the output of the transducer can be written as:

$$X_{out}(T) = X_{out}(T_0) + (\alpha_R - \alpha_{GMR})(T - T_0)x_{in} \qquad (10)$$

Here, according to our convention, x_{in} changes from 0 to $\pm \frac{\text{Range}}{2}$. That means that at the center position when the bridge is completely balanced, the output of the transducer is independent from temperature variations. The worst temperature dependence should occur at the ends of the range. Thermal coefficients of resistance for Ni and Fe are 0.0065 1/C, and for Cu is 0.0038 1/C. Using these values we can estimate $\alpha_{transducer} \approx$ (0.002 -- 0.004) 1/C and expect thermal drift at the ends of the range to be about (25 -- 50) μm/C.

Test set-up

In or experiments we used two precision linear position calibrators. One was designed and built by OPTRA, Inc., Topsfield, MA. This unit used OPTRA's optical scale. Another one was designed and built by Federal Products Co, Providence, RI. This unit used Micro-E, Inc., Natic, MA optical encoder. Both calibrators utilized precision air slides and provided accuracy of positioning on the nanometer level.

From electrical stand point we used two different techniques AC and DC. In AC approach we used EG&G Lock-in Amplifier, model 7260. For the DC measurements Keithley Microohm meter, model 580 was used.

Temperature dependence of GMR transducers was studied with the help of Tenney Environmental Chamber, model TUJR. Temperature was measured with ERTCO-Hart thermometer equipped with standard Pt probe, model 850.

Noise measurements in part were done with HP 89410A Vector Signal Analyzer.

The maximum field in the gap of magnet assembly was measure with Gaussmeter GM1A from Applied Magnetics Laboratory, Inc.

Results and Discussion

GMR resistors were fabricated on the 4" diameter Si wafer by sputtering technique. Then resistors were diced, tested, assembled, and wire bonded. GMR resistors with nominal resistance 100, 380, 800 and 5000 Ohm were tested. On early stages of work it was found that elements with 380 Ohm resistance provided better combination of sensitivity and signal-to-noise ratio. These particular resistors were selected for further testing and provide data presented here.

Initially we worked in AC domain, hoping to avoid 1/f-noise, which was believed to be major component of the noise in GMR resistors at low frequencies. We conducted tests at 1, 5 10, 20 and 50 kHz varying excitation level between 10 mV and 10 V. It was found that AC method did not actually provide better signal-to-noise ratio compare to DC technique.

In DC domain we used 1 mA constant current, pulsed with frequency 3 Hz in order to decrease self heating. Resistance was measured during 165 ms pulses by 4-probe technique. It turned out that this method being more economical and easy to use, also provided more reliable data with better resolution than AC technique, and was used on final stages of testing. However, results obtained by DC and AC techniques were consistent.

During this work we assembled and tested more than a dozen of GMR transducers. In many cases we will refer to data obtained from a particular transducer #ZZZ, which being a "good" sensor still is a "good representative" of merits and problems occurring throughout the whole ensemble.

Characterization of the GMR transducers included studying several metrological parameters: linearity, resolution, hysteresis, repeatability and thermal susceptibility.

Linearity, Hysteresis and Repeatability

Linearity is important parameter of a displacement transducer. Deviation from linear response can be corrected in some extent[i], however, it leads to increasing the price of the product and should be avoided if possible. The full range of our transducers was 23 mm. We measured linearity over full range, 8 mm range and 1 mm range. The least square linear fit function provided by MS Excel was used and deviations from obtained straight line were plotted and analyzed. Typical results are shown in the Fig. 7 -- 10. Metrological parameters summarized in the Table 1.

Figure 7 shows typical response functions for the transducers utilizing 176^o, 132^o, 88^o and 44^o central angle magnets. Curves were off-set from each other along vertical axis to provide clear viewing. Pronounced deviations from linearity at the ends of the range go in accord with the theoretical model developed above, Figure 6 (b). We found[13] that devices equipped with 88^o central angle magnets had generally better linearity and hysteresis.

Hysteresis is a crucial parameter for linear position transducer. Essentially hysteresis and not deviation from linearity dictates ultimate accuracy of the device. We measured hysteresis by completing two full cycles of the displacement: forward (FW1) – backward (BW1) – forward (FW2) – backward (BW2). Linear fit was obtained for the full set of data from two cycles. Deviation from linearity reveals the presence of hysteresis.

Measured values of hysteresis for magnets with 176^o, 132^o and 88^o central angle, respectively, were 44, 55 and 5 μm, Figure 7. The maximum values estimated above and due solely to the GMR effect were 16, 12, 9 μm. These values should be independent on the length of the test stroke and location of the stroke within the working range of the transducer. In reality, though, the values of hysteresis were much bigger than estimated. The more so, hysteresis tends to be larger for the longer strokes. In addition to that, some transducers demonstrated "steps" and "plateaus" in their response curves and extremely large hysteresis values associated with those abnormalities. One of those is shown in Figure 7 for 44^o magnets. The phenomenon is very repeatable (two hysteresis loops overlap almost exactly) and reproducible. Six transducers from ten tested showed similar anomalies. We associate these anomalies with defects in GMR structures. Figure 11 shows variations in the nominal values of resistance and GMR ratios cross the wafer of elements. Resistance is quite uniform across the wafer. All variations are within 1% range. However, GMR ratio varies a lot from element to element -- up to 10%! Two adjacent resistors were just 1 mm apart and their values, of course, are the average along the length of the resistor. So we can reasonably assume that there are substantial local variations of the GMR ratio along longitudinal axis of the GMR stripe. For example, slight variations in the thickness of Cu buffer layer will result in variations of coupling between magnetic layers, and, consequently, in variations of GMR ratio.

---

[i] Federal Products Co. manufactures μMaxum™ electronic dial indicator. Without linearization the range of the device is 1 mm with maximum deviation from linearity $\pm$1%. After linearization through 3rd degree polynomial fit, the linearity has been improved up to $\pm$0.25%.

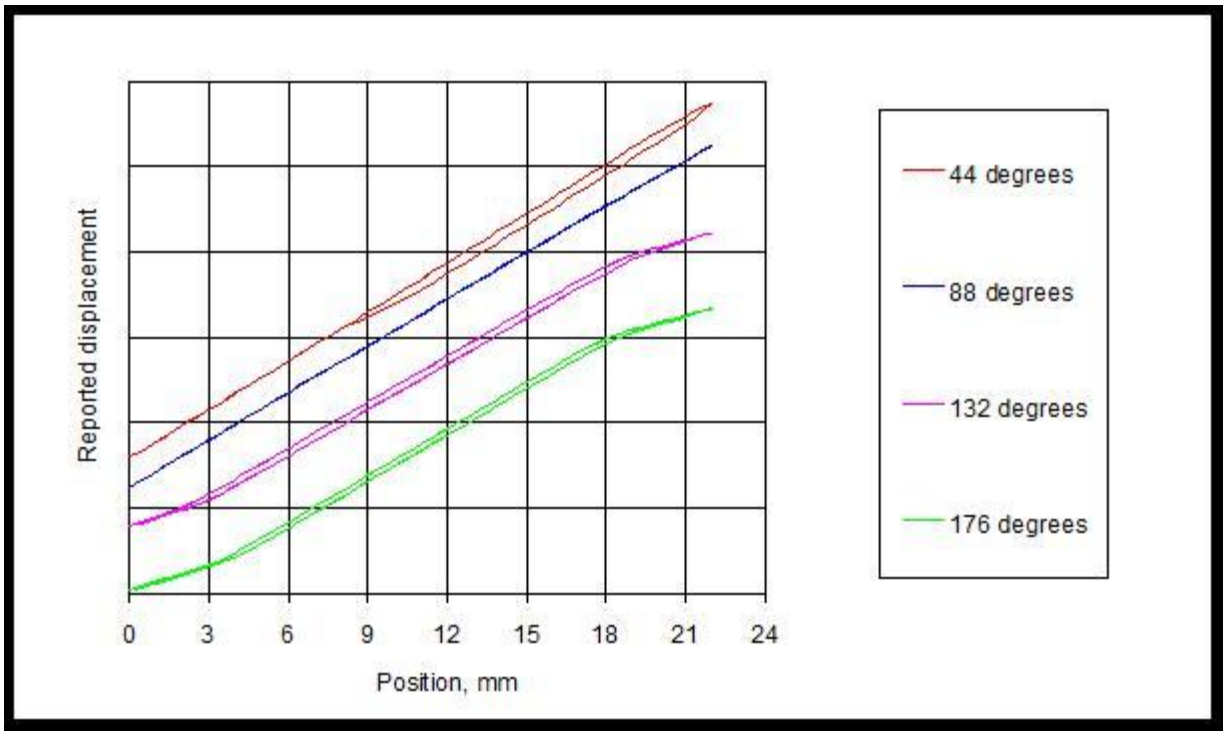

Figure 7.Experimental data from sensor #ZZZ with four magnets 44°, 88°, 132° and 176° central angle in the "friction-free" configuration. Two "forward-backward" cycles are shown. Delay between sampling is 5 sec. Curves are off-set to provide better viewing

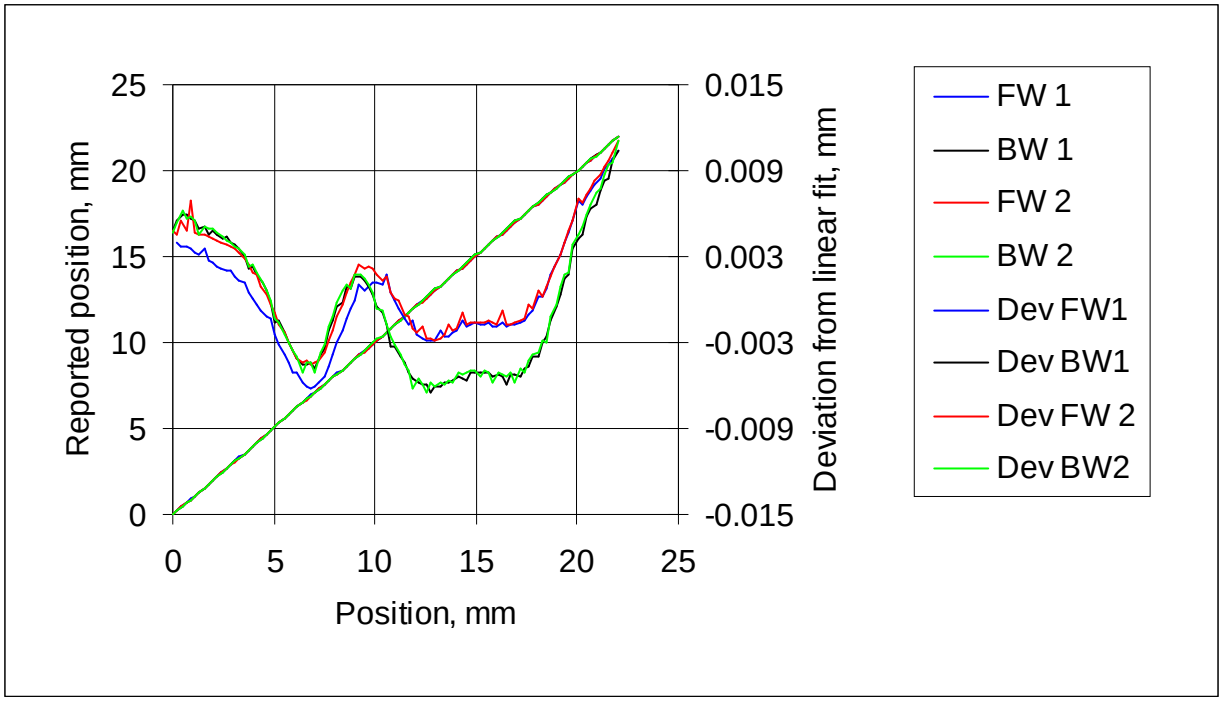

Figure 8. Best achieved results with GMR sensors. ZZZ sensor with 88° magnets in the "friction-free" configuration. Two "forward-backward" cycles are shown. Step is 0.23 mm. Delay between sampling is 5 sec. Sensitivity is 0.91 Ohm/mm.

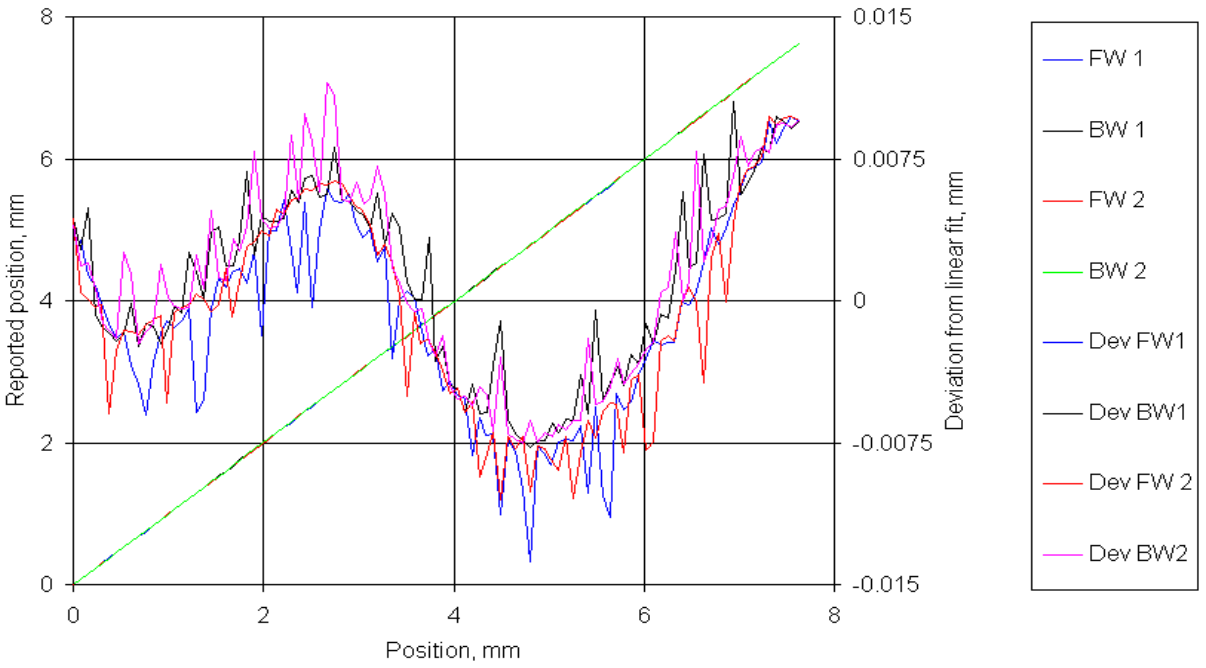

(a)

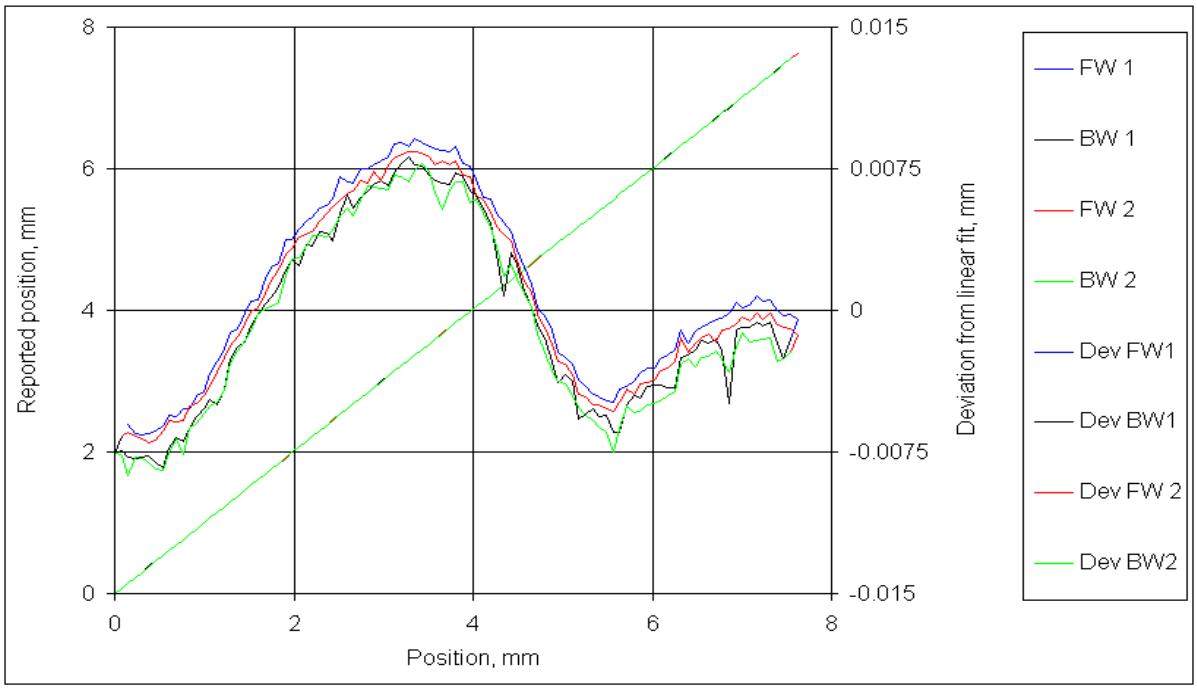

(b)

Figure 9. Sensor #ZZZ with 44° magnets. 8 mm range. Initial position is at 7 mm of 23 mm full range. Two forward (FW)-backward (BW) cycles are shown. Step is 0.08 mm. Sensitivity is 0.9 Ohm/mm. (a) -- delay between sampling is 2 sec, (b) -- delay between sampling is 5 sec.

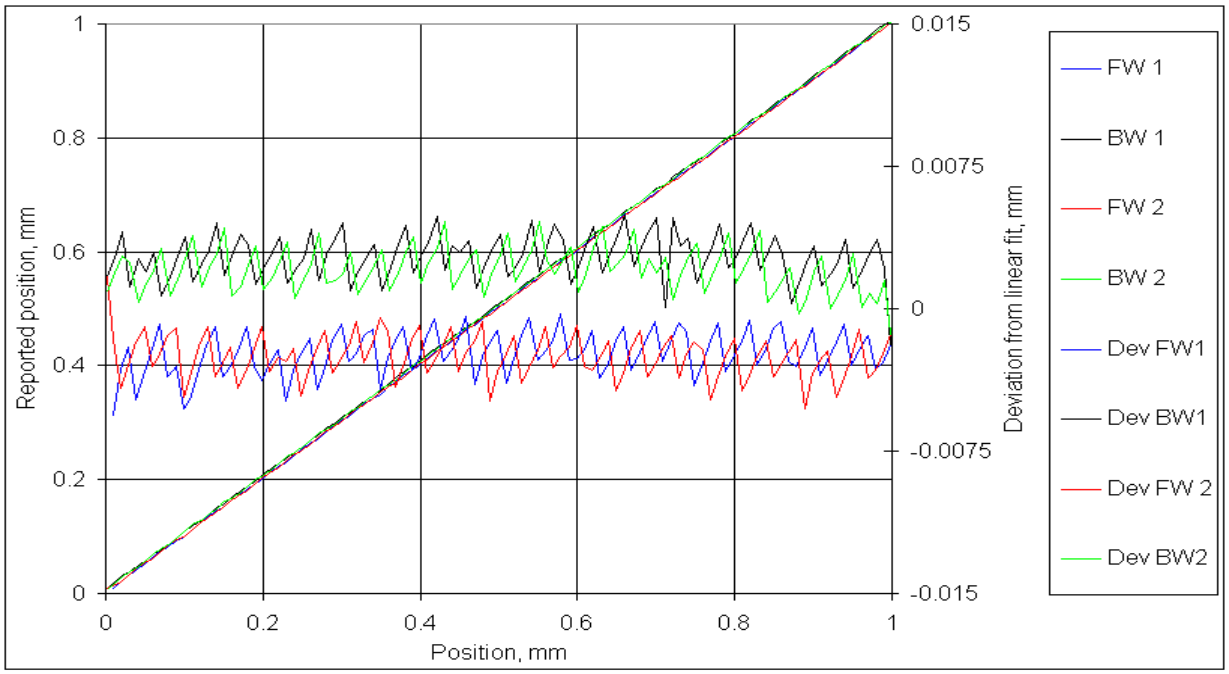

(a)

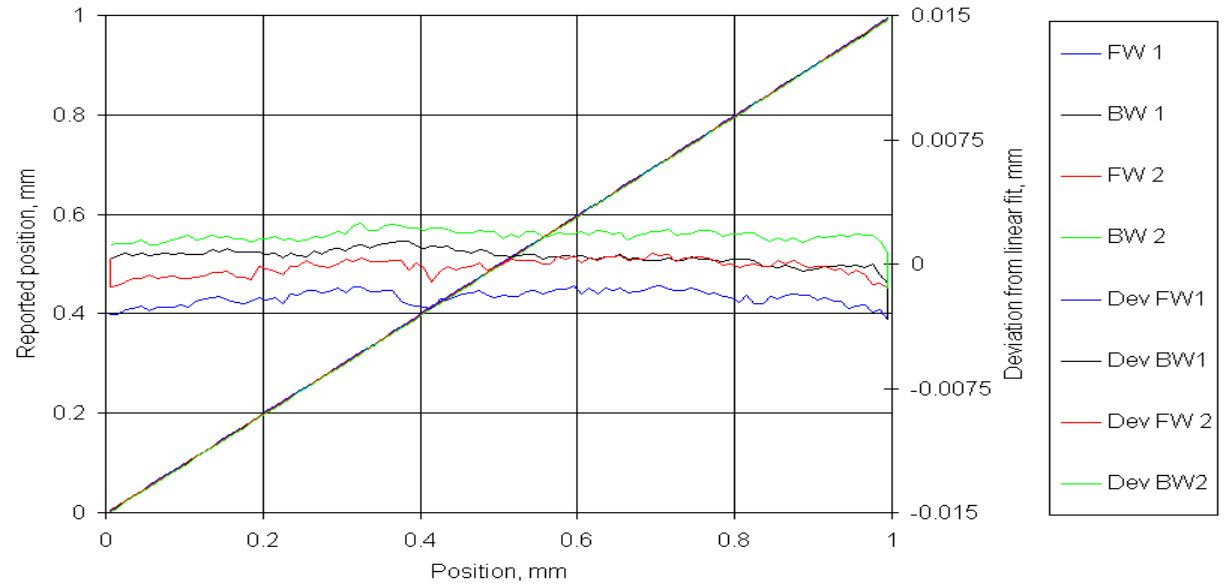

(b)

Figure 10. Sensor #ZZZ with 44° magnets represents typical linearity and hysteresis of the GMR sensors. 1 mm range. Initial position is at 8 mm of 23 mm full range. Two forward (FW)-backward (BW) cycles. Step is 10 μm. Sensitivity is 0.9 Ohm/mm. (a) -- delay between sampling is 2 sec, (b) -- delay between sampling is 10 sec

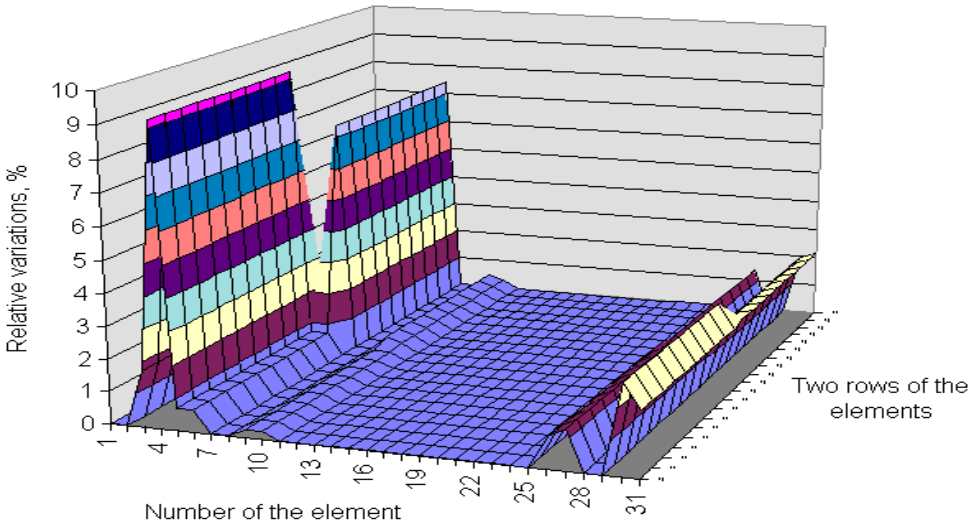

(a)

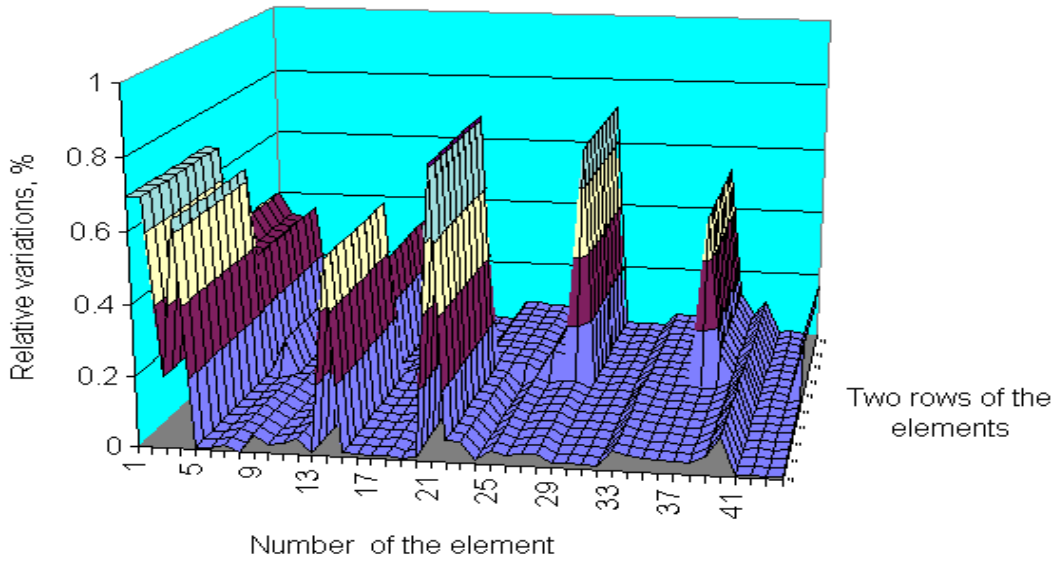

(b)

Figure 11. Relative variations in parameters of the GMR resistors across the wafer. (a) -- GMR ratio. Only 26 resistors located at the ends of each row were tested. Flat area in the middle represents no data. (b) -- Resistance.

Response time, Relaxation and Demagnetization

Deviation from linearity curves obtained on 8 mm range test, Figure 9 (a), have many spikes which appear to be "noise". However, all spikes occurred on motion "forward" point down and all spikes occurred on motion "backward" point up. We tested the transducer in the "friction-free" mode, when magnet assembly was attached directly to the calibrator and did not slide on the V-groove of the transducer housing. This test demonstrated the same effect. Similar results were obtained from tests conducted on different

calibrators. That leads us to conclude that this effect was caused neither by friction in the transducer, nor by inaccuracy of calibrators.

Table 1. Some metrological parameters of GMR based linear position transducer (unit #ZZZ) with 88° central angle magnets

Resolution (MDS), 1 σ, 4 Hz update rate, μm	Thermal coefficient, ppm/°C	Deviation from linearity, μm			Hysteresis, μm		
		23 mm range	8 mm range	1 mm range	23 mm range	8 mm range	1 mm range
0.2	**2200**	**10**	**10**	**5**	**5**	**2**	**3**

We noticed also that at some positions of the magnets the output reading keeps changing after calibrator has arrived on the prescribed position. The bridge resistance reached stable value only after several seconds. Figure 9 (b) shows results of the similar test with 5 sec delay between sampling. Significant reduction in number of spikes can be observed. Five transducers exhibited very long (about 20 min.) relaxation constant in some positions. Similar results were observed on 1 mm range tests, Figure 10.

This relaxation effect is a serious issue and undermines the whole concept of the transducer. The fundamental assumption of the transducer functioning is that the flipping layer possesses enough coercivity in order to retain its state of magnetization even when magnet assembly is all the way in- or out, i.e., at the ends of the range. The existence of relaxation process, shown in Figure 12, suggests that it is not happening.

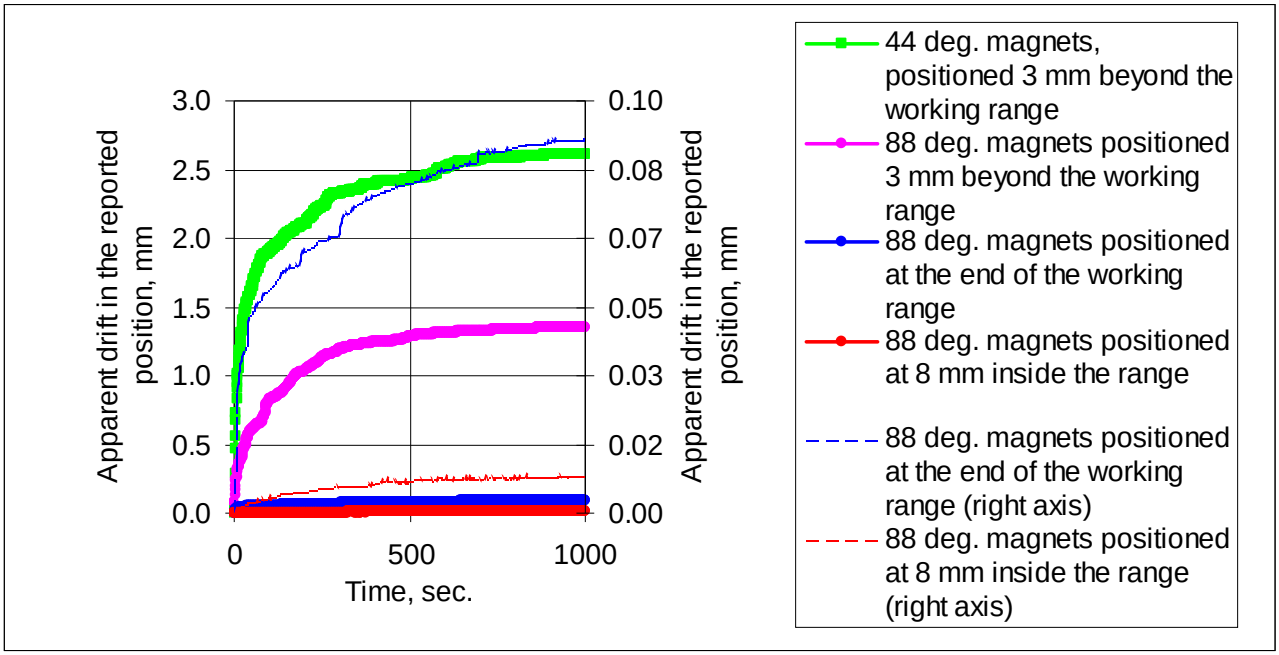

Figure 12. Relaxation observed in the GMR transducers. Sensor # ZZZ with 44° and 88° magnets. 1 hour test. Sampled every 3.6 sec

Even a "good" transducer #ZZZ exhibits a significant relaxation when magnet assembly positioned beyond the working range of the transducer. For example, when 44^o magnets were positioned approximately 3 mm beyond the working range, this relaxation led to the drift in reported position of about 2.5 mm during 1 hour test. We found that the degree of relaxation is inversely proportional to the strength of the magnetic field and directly proportional to the area of the sensor not covered by the magnetic field. When 44^o magnets were substituted with 88^o magnets, the drift was reduced to about 1.5 mm. In case when 88^o magnets were positioned at the edge of the range the drift was reduced to about 0.1 mm. After 88^o magnets were moved at position about 8 mm inside the working range, the drift had been reducer further to 0.01 mm and stable state had been reached within 10 min.

We interpret these results in terms of demagnetization processes taking place in the GMR films subjected to the room temperature and "zero" magnetic field. The rule of thumb[14] is that at the room temperature the thermal energy is sufficient enough to switch uniform magnetization of the particle with length under 0.1 μm. Suppose an assembly of such particles is magnetized in the same direction by the application of a suitable large magnetic field, which is then turned off. The magnetization spontaneously decays according to:

$$M(t) = M(t_0)\exp\left(\frac{-t}{\tau}\right), \tag{11}$$

where τ is relaxation time. The relaxation time can be estimated as following:

$$\tau = 10^{-9} \exp\left(\frac{0.5 M_s H_c v}{kT}\right) \tag{12}$$

where k is Boltzman's constant, T is the absolute temperature, M_s is the saturation magnetization, H_c is the coercive force and v is the volume of a particle. Because of the exponential form of Eq. (12), the relaxation time changes very rapidly with changing the particle size. For example, if the dimensions of a 100-second particle are increased by only 20%, the volume increases by 1.2 cubed, and the relaxation time becomes over 100 years. Practically, this means that, when a group of particles has a wide distribution of sizes, there exists, at any temperature, a clear-cut boundary between those which are stable single-domain particles and those which are thermal idiots.

Variations in the thickness of layers, discussed above, can lead to creation "islands" in magnetic layers, with different type and/or strength of coupling. These "islands" can be responsible for "steps and plateaus" on the transducer transfer functions, for the abnormal hysteresis associated with them, and for the described relaxation processes. Although GMR films used here were continuous, they probably should be thought of as closely packed assembly of single-domain grains[15].

Relaxation reported above has been observed and recorded one and a half year after GMR films were manufactured. We believe that this effect was either not that pronounced earlier and could be masked by thermal drift, or it, possibly, was not present at all. All layers in the GMR structures were only 15 -- 70 A thick. It is possible that interlayer diffusion played some role here, as well..

Of course, all these processes are not desirable in linear position transducer. We believe, that they can be minimized either through manufacturing the GMR layers with more uniform thickness and more homogeneous properties, or through design that will ensure presence of strong enough magnetic field at all parts of the transducer, regardless where magnets are.

Noise and Resolution

We define Minimum Detectable Signal (MDS) as a signal equal to 1 σ (1 standard deviation) and will regard resolution as MDS. From linearity and hysteresis measurements, Figure 10 (b), MDS can be estimated to be approximately 0.1 μm. MDS can also be derived from the noise measurements. Noise in the output signal of transducers was assessed by acquiring data during 1 hour test with sampling every 3.6 sec. Probe of the transducer was locked during this test. Typical results are shown in the Figure 13. Initial drop on the signal is the relaxation mentioned above. Characteristic time is about 2 min. The following drift in the signal is caused by decrease of the temperature. Temperature dependence coefficient derived from this drift is 0.00057 1/C. This value is about 3 times smaller than value obtained from dedicated temperature dependence measurements (see below). Difference is probably due to inaccuracy associated with very small temperature variations that occurred during this experiment. It is obvious, that after removing this thermal drift we reach the digitization limit of the micro-ohm meter. Scaled to the displacement it was 0.1 μm (for these particular transducers having sensitivity of about 0.9 Ohm/mm).

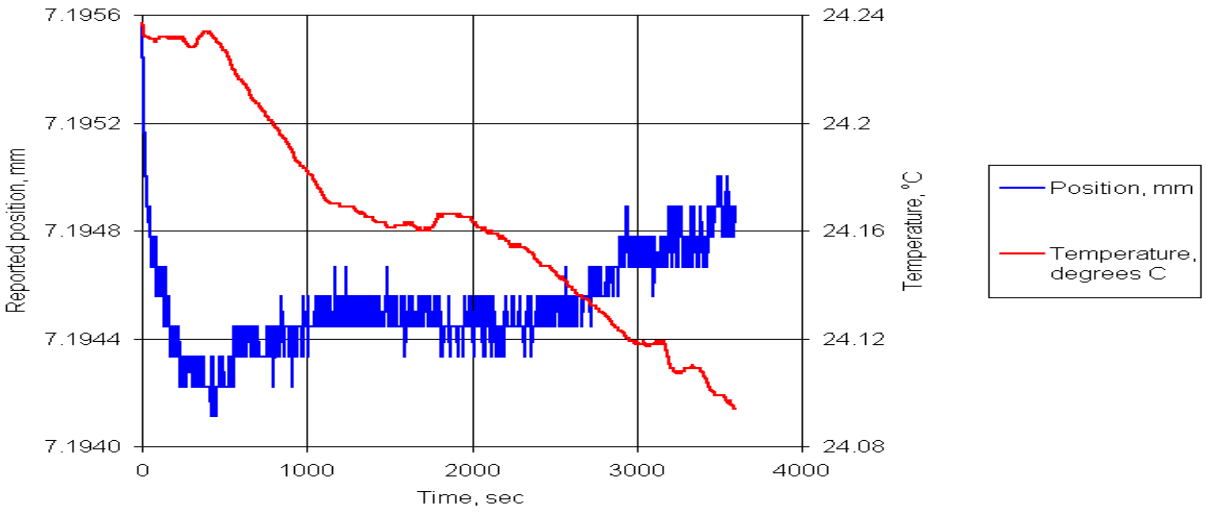

Figure 13. Noise in the output signal of GMR sensor # ZZZ with 44° magnets positioned at about 7 mm inside the working range. 1 hour test, sampled every 3.6 sec. Initial drop in the signal is the relaxation discussed in the text. Thermal drift can be observed. a = 0.00057 1/°C

The nature of noise in GMR structures is still in question. The most measurements show that it is about an order of magnitude higher than that in the regular resistors of the same value. Mostly accepted hypothesis is that additional noise comes from processes happening on the edges of GMR films. It has been shown[16] that for the resistor of rectangular shape, the increase in ratio of the perimeter to area leads to increase of noise. Random thermal demagnetization processes discussed above, certainly can contribute to the observed noise. Higmore et. al.[17] put forward horizontal antiphase domain boundaries (ADBs) as the most influential magnetic defects in the multi-layer structures with ferromagnetic -- antiferromagnetic coupling. They demonstrate that ADBs can be responsible for $GMR_{observed}$ to be smaller than GMR_{ideal}. They calculate GMR_{ideal} to be equal to 66% (world's record GMR ratio is 65% since 1991[2, 3]). They also suggest that horizontal ADBs are stabilized by fluctuations in Cu layer thickness, which cause the magnitude and even the sign of the inter-layer exchange coupling to vary within a multi-layer structure.

Because the resolution of the sensor is very important parameter, noise in the transducers was also measured with spectrum analyzer. Typical noise density spectrum is shown in the Figure 14 for the frequency range 0 -- 1 kHz. Typical noise density for our transducers was approximately 60 $nV_{rms}/\sqrt{Hz}$, which allows 0.2 μm resolution with a 4 Hz update rate. This value corresponds to MDS values reported above and obtained through different techniques.

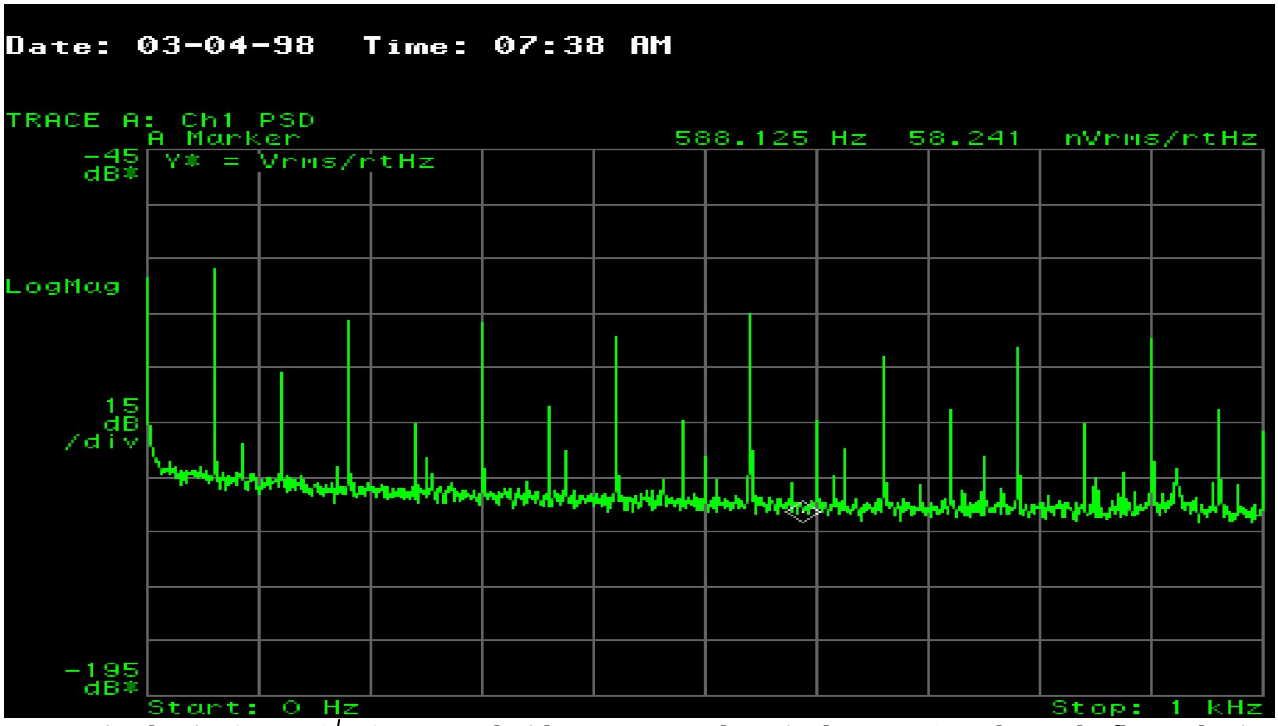

Figure 14. Noise density (nVrms/√Hz) measured with spectrum analyzer in the range 0 -- 1 kHz. The floor value is approximately 60 nVrms/√Hz, which translates into 0.2 μm resolution with a 4 Hz update rate

Temperature Dependence

Temperature dependence was studied in the interval 25 -- 45 ^{o}C and is shown in Figure 15. The signal varies linearly with temperature. Temperature dependence coefficient α has been determined to be (0.0022 $\pm$ 0.00085) 1/^{o}C, which corresponds to the simple model, Eq. (10). The thermal drift of the reported values of displacement at the edges of the range is 35 μm/^{o}C.

Conclusions

This paper describes the design, model and test results of GMR-based linear position sensor. The transducer was packaged in a 12 x 2 x 2 cm housing. It is shown that both GMR and AMR effects have to be taken into account to model correctly the output of transducer. It has been found that indexing magnets with 88^{o} central angle provide the best characteristics among tested magnets.

The sensitivity of the sensor was approximately 1 Ohm/mm. The best achieved deviation from linearity over a range of 23 mm was $\pm$10 μm ($\pm$0.05% of full scale), with hysteresis of 5 μm. Noise density of the transducer was 60 $nV_{rms}/\sqrt{Hz}$, which allows 0.2 μm resolution with a 4 Hz update rate. Sensor's output varies linearly with temperature (α = 0.0022 1/^{o}C). It is proportional to the measured displacement,

which scales to 35 μm/°C at the ends of the working range. This is probably unacceptable in most applications and some auto-compensation method should be developed.

Relaxation processes in the GMR structure have been observed. It is found that they can be minimized by choosing correct magnets. This effect has been discussed in conjunction with non-linearity and abnormal hysteresis sometimes observed in the transducers, as well as noise. It is suggested that non-uniformity in thickness of the GMR layers as well as defects can be held responsible for these anomalies.

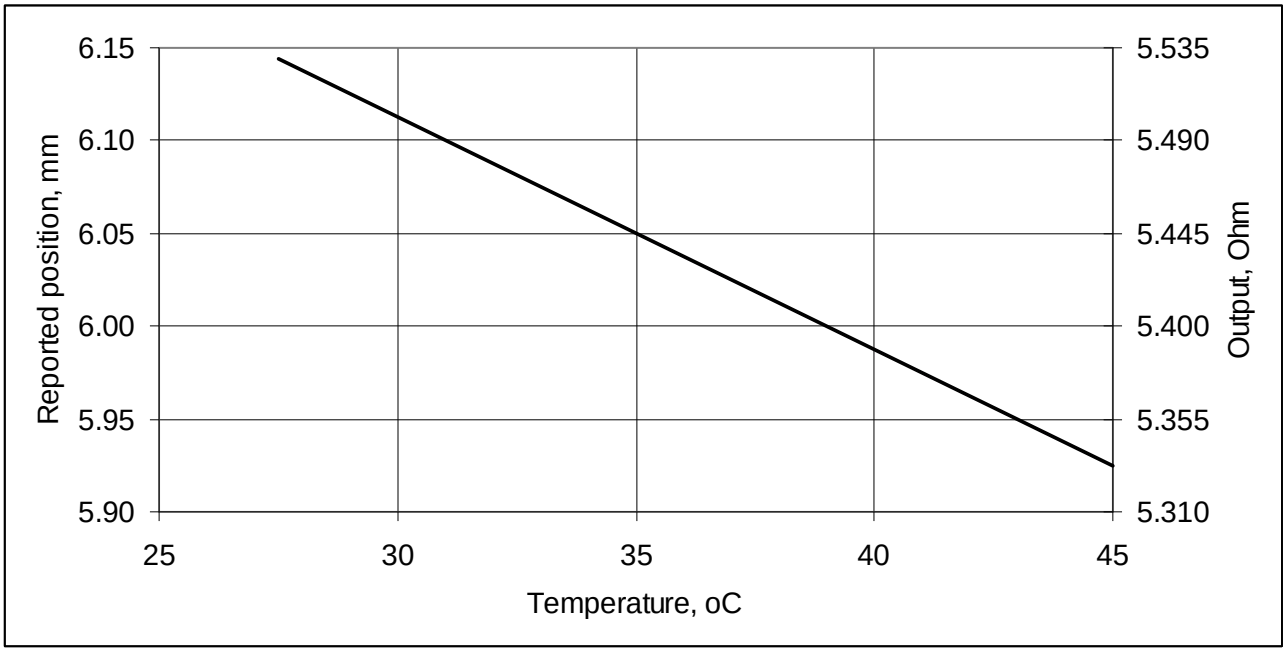

Figure 15. Temperature dependence of the output of GMR sensor #ZZZ with 44° magnets positioned about 6 mm inside the working range. α= 0.0022 1/°C

Acknowledgments

This work was done as a part of a consortium studying applications of GMR materials. Consortium members included Nonvolatile Electronics, Inc. (NVE), Honeywell, Inc., Naval Research Lab (NRL), and Hughes Research. Consortium efforts were supported by the individual members of the consortium and by DARPA.

We appreciate the contributions of many people from Federal Products. In particular, Carl North was responsible for mechanical design of the transducer, Chih Hua Hsu designed the precision calibrator, Gurpreet Singh helped us with LabView and Jon Klinkhammer was involved in characterization of the transducers.

We also very grateful to Jim Daughton and Carl Smith from NVE, Hong Wan and Lucky Wiphanawsam from Honeywell, Gary Prinz, Peter Lubitz and Mike Miller from NRL and Stu Smith from UNCC for useful discussions on all stages of work.

References

[1] Baibich, M.N., Broto, J.M., Fert A., et.al., "Giant Magnetoresistance of (001)Fe/(001)Cr Magnetic Superlattices", *Phys. Rev. Lett.*, 1988, **61**, 21.

[2] Mosca, D.H., Petroff, F., Fert, A., et. al., *J. Magn. and Magn. Mat.*, 1991, **94**, L1-L5.

[3] Parkin, S.S.P., Li, Z.G., Smith, D.J., *Appl. Phys. Lett*., 1991, **58**, 2710.

[4] Dieny, B., Speriosu, V.S., Parkin, S.S.P., et. al., " Giant Magnetoresistance in Soft Ferromagnetic Multilayers", *Phys. Rev*., 1991, **B43**, 1.

[5] Prinz, G., "Magnetoresistive linear displacement sensor, angular displacement sensor, and variable resistor using a moving domain wall", *U.S. Patent 5,475,304*, 1995.

[6] Shuhl, A., Tyc, S., "Sensor of weak magnetic fields, with magnetoresistive effect", *U.S. Patent 5,313,186*, 1994.

[7] Smith, N., Zeltser, A., Yang, D.L., Koeppe, P.V., "Very High Sensitivity GMR Spin-Valve Magnetoneter", INTERMAG'97, April 1-4, New Orleans, LA, USA.

[8] Heremans, J.P., "Solid-State Magnetic Hield Sensors and Applications", General Motors Research Publications, 1993, GMR-7895.

[9] Prinz, G., "Spin-Polarized Transport", *Physics Today*, 1995, 58-63.

[10] Mallinson, J.C. *Magneto-Resistive Heads, Fundamentals and Applications*. San-Diego: Academic Press, 1996.

[11] Blakemore, J.S. *Solid State Physics*, Cambridge, UK: Cambridge University Press, 1988

[12] Chaiken, A., Gutierrez, C.J., Krebs, J.J. and Prinz, G.A., "Composition dependence of gaint magentoresistance in Fe/Ag/Co_xFe_{1-x} sandwiches", *J. Magn. Mag. Mater.*, 1993, **125**.

[13] Tchertkov, I., Klinkhamer, J., "Magnetoresistive Displacement Sensor", Application for the U.S. Patent. Application number 08/772723, filing date 12/23/96.

[14] Mallinson, J.C. *The Foudations of Magnetic Recording*, San-Diego: Academic Press, 2nd Edition. 1993

[15] Hylton, T.L., Coffey, K.R., Parker, M.A., Howard, J.K., "Giant Magnetoresistance at Low Fields in Discontinuos NiFe-Ag Multilayer Thin Films", *Science*, 1993, **261**, 1021-24.

[16] GMR Consortium, 6th Quarterly Review, 1997.

[17] Higmore, R.J., Evetts, J.E. and Somekh, R.E., "Magnetic defects in antiferromagnetically-coupled Co-Cu multileyers", *J. Magn. and Mag. Mater.*, 1993, **123**, L13-L17